

Elliptic flow and freeze-out from the parton cascade MPC

Dénes Molnár and Miklos Gyulassy^{a*}

^aPhysics Department, Columbia University
538 West 120th Street, New York, NY 10027, U.S.A.

Differential elliptic flow out to $p_{\perp} \sim 5$ GeV/c and particle spectra are calculated using the MPC elastic parton cascade model for Au+Au at $E_{cm} \sim 130$ A GeV. The evolution is computed from parton transport theory, followed by hadronization either via independent fragmentation or by imposing parton-hadron duality. With pQCD elastic cross sections, very large initial gluon densities $dN_g/d\eta > 7000$ are required to reproduce the data measured by the STAR collaboration. In addition, elliptic flow and the p_{\perp} spectra are shown to be very sensitive to particle subdivision.

1. Introduction

Elliptic flow, $v_2(p_{\perp}) = \langle \cos(2\phi) \rangle_{p_{\perp}}$, the differential second moment of the azimuthal momentum distribution, has been the subject of increasing interest [1–5], especially since the discovery[6] at RHIC that $v_2(p_{\perp} > 1 \text{ GeV}) \rightarrow 0.2$. This sizable high- p_{\perp} collective effect depends strongly on the dynamics in a heavy ion collision and provides important information about the density and effective energy loss of partons.

The simplest theoretical framework to study elliptic flow is ideal hydrodynamics[1]. For RHIC energies, ideal hydrodynamics agrees remarkably well with the measured elliptic flow data[6] up to transverse momenta ~ 1.5 GeV/c. However, it fails to saturate at high $p_{\perp} > 2$ GeV as does the data reported by STAR at Quark Matter 2001.

A theoretical problem with ideal hydrodynamics is that it assumes local equilibrium throughout the whole evolution. This idealization is marginal for conditions encountered in heavy ion collisions[7]. A theoretical framework is required that allows for nonequilibrium dynamics. Covariant Boltzmann transport theory provides a convenient framework that depends on the local mean free path $\lambda(x) \equiv 1/\sigma n(x)$.

Parton cascade simulations[2,3] show on the other hand, that the initial parton density based on HIJING[8] is too low to produce the observed elliptic flow unless the pQCD cross sections are artificially enhanced by a factor $\sim 2 - 3$. However, gluon saturation models[9] predict up to five times higher initial densities, and these may be dense enough to generate the observed collective flow even with pQCD elastic cross sections. In this study, we explore the dependence of elliptic flow on the initial density and the elastic gg cross section.

*This work was supported by the Director, Office of Energy Research, Division of Nuclear Physics of the Office of High Energy and Nuclear Physics of the U.S. Department of Energy under contract No. DE-FG-02-93ER-40764.

Calculations based on inelastic parton energy loss[4] also predict saturation or decreasing v_2 at high p_\perp . These calculations are only valid for high p_\perp , where collective transverse flow from lower- p_\perp partons can be neglected. The collective component from low p_\perp is, on the other hand, automatically incorporated in parton cascades. Though parton cascades lack at present covariant inelastic energy loss, elastic energy loss alone may account for the observed high- p_\perp azimuthal flow pattern as long as the number of elastic collisions is large enough [3].

Forerunners of this study [2,3] computed elliptic flow for partonic systems starting from initial conditions expected at RHIC. Here, we extend these in three aspects. We compute the p_\perp -differential elliptic flow $v_2(p_\perp)$, model hadronization, which enables us to compute the final observable hadron flow, and consider realistic nuclear geometry.

2. Covariant parton transport theory

We consider here, as in [3,7,10,11], the simplest form of Lorentz-covariant Boltzmann transport theory in which the on-shell phase space density $f(x, \mathbf{p})$, evolves with an elastic $2 \rightarrow 2$ rate. We solve the transport equation using the cascade method, which inherently violates Lorentz covariance. To ensure Lorentz covariance, we apply the parton subdivision technique[10,12]. See [7] for details.

The elastic gluon scattering matrix elements in dense parton systems are modeled by a Debye-screened form $d\sigma/dt = \sigma_0(1 + \mu^2/s)\mu^2/(t - \mu^2)^2$, where μ is the screening mass, $\sigma_0 = 9\pi\alpha_s^2/2\mu^2$ is the total cross section, which we chose to be independent of energy.

3. Numerical results

The initial condition was a longitudinally boost invariant Bjorken tube in local thermal equilibrium at $T_0 = 700$ MeV at proper time $\tau_0 = 0.1$ fm/ c as by fitting the gluon mini-jet transverse momentum spectrum predicted by HIJING[8] (without shadowing and jet quenching). The pseudo-rapidity distribution was taken as uniform between $|\eta| < 5$, while the transverse density distribution was assumed to be proportional to the binary collision distribution for two Woods-Saxon distributions. For collisions at impact parameter b , the transverse binary collision profile is $dN_g(\mathbf{b})/d\eta d^2\mathbf{x}_\perp = \sigma_{jet}T_A(\mathbf{x}_\perp + \mathbf{b}/2)T_A(\mathbf{x}_\perp - \mathbf{b}/2)$, where $T_A(\mathbf{b}) = \int dz \rho_A(\sqrt{z^2 + \mathbf{b}^2})$, in terms of the diffuse nuclear density $\rho_A(r)$. From HIJING, the pQCD jet cross section normalization at $b = 0$, σ_{jet} is fixed such that $dN(0)/d\eta = 210$.

The evolution was performed numerically with 40 and 100 mb isotropic cross sections, and with 3, 40 and 100 mb gluonic cross sections ($\mu = T_0$). We used particle subdivision $\ell = 100$ for impact parameters 0, 2, and 4 fm, while $\ell = 220, 450, 1100$, and 5000, for $b = 6, 8, 10$, and 12 fm.

Two different hadronization schemes were applied. One is based on local parton-hadron duality, where as [9], we assumed that each gluon gets converted to a pion with equal probability for the three isospin states. Hence, $f_{h^-}(\mathbf{p}_\perp) \approx f_{\pi^-}(\mathbf{p}_\perp) = \frac{1}{3}f_g(\mathbf{p}_\perp)$.

The other hadronization prescription was independent fragmentation. We considered only the $g \rightarrow \pi^\pm$ channel with the NLO fragmentation function from [13]. For the scale factor $s \equiv \log(Q^2)/\log(Q_0^2)$ we take $s = 0$ because the initial HIJING gluon distribution is already quenched due to initial and final state radiation. Since we do not consider soft

physics, we limit our study to hadrons with $p_{\perp} > 2$ GeV.

Due to scaling [7], differential elliptic flow depends on σ_0 and $dN_g/d\eta$ only via $\xi \equiv \sigma_0 dN_g(0)/d\eta$. On the other hand, the p_{\perp} spectrum depends on σ_0 and $dN_g/d\eta$ *separately*.

3.1. Elliptic flow results

Fig. 1 shows elliptic flow as a function of p_{\perp} and impact parameter. With increasing p_{\perp} , the minimum-bias elliptic flow increases until $p_{\perp} \sim 1.5 - 2$ GeV, where it saturates. With increasing impact parameter, elliptic flow first monotonically increases, then monotonically decreases, showing a maximum at $b \approx 8$ fm.

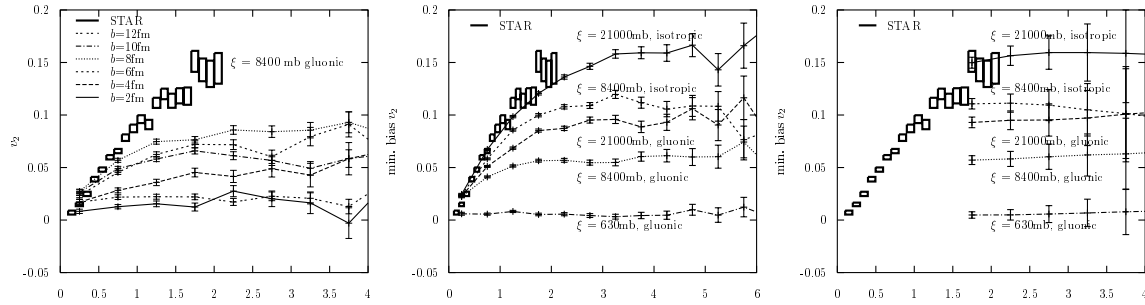


Figure 1. Elliptic flow as a function of p_{\perp} for Au+Au at $\sqrt{s} = 130A$ GeV. Left figure shows gluon elliptic flow for different impact parameters. Middle and right figures show *minimum-bias* charged hadron v_2 for hadronization via local parton-hadron duality (middle) or independent fragmentation (right).

The minimum-bias flow was computed via $v_2^{m.b.}(p_{\perp}) \equiv \frac{2\pi}{\pi b_{max}^2} \int_0^{b_{max}} v_2(b, p_{\perp}) b db$, where we chose $b_{max} = 12$ fm. This differs from the definition by STAR, which weights $v_2(b, p_{\perp})$ with $dN_g/dydp_{\perp}$ and hence results in a smaller $v_2(p_{\perp})$ than our estimate.

The $\xi = 8400$ mb isotropic curve is almost the same as the $\xi = 21000$ mb gluonic curve, showing that not the *total*, rather the *transport* cross section is the relevant parameter. Thus, we expect that the flow in the $\xi = 21000$ mb isotropic case can also reproduced with $\xi \sim 50000$ mb and a gluonic cross section. With the pQCD gg cross section of 3mb, this corresponds to an 80 times larger initial density than from HIJING.

3.2. Particle spectra

Fig. 2 shows the quenching of the p_{\perp} spectra due to elastic energy loss. In the dilute $\xi = 630$ mb case quenching is negligible, however, for $\xi = 21000$ mb it is an order of magnitude at $p_{\perp} > 6$ GeV for semicentral collisions. Naturally, for a fixed ξ , quenching decreases as the collision becomes more peripheral because the parton density decreases. Hadronization via independent fragmentation results in an additional quenching.

Fig. 3 shows that elliptic flow and the p_{\perp} spectra are sensitive to particle subdivision. To obtain covariant results for these conditions, we needed $\ell > 200$.

REFERENCES

1. P. F. Kolb, P. Huovinen, U. Heinz and H. Heiselberg, hep-ph/0012137; P. Huovinen, P. F. Kolb, U. Heinz, P. V. Ruuskanen and S. A. Voloshin, hep-ph/0101136.
2. B. Zhang, M. Gyulassy and C. M. Ko, Phys. Lett. **B455**, 45 (1999) [nucl-th/9902016].
3. S. A. Bass *et al.*, Nucl. Phys. **A661**, 205 (1999) [nucl-th/0005051]; D. Molnar and M. Gyulassy, nucl-th/0102031.

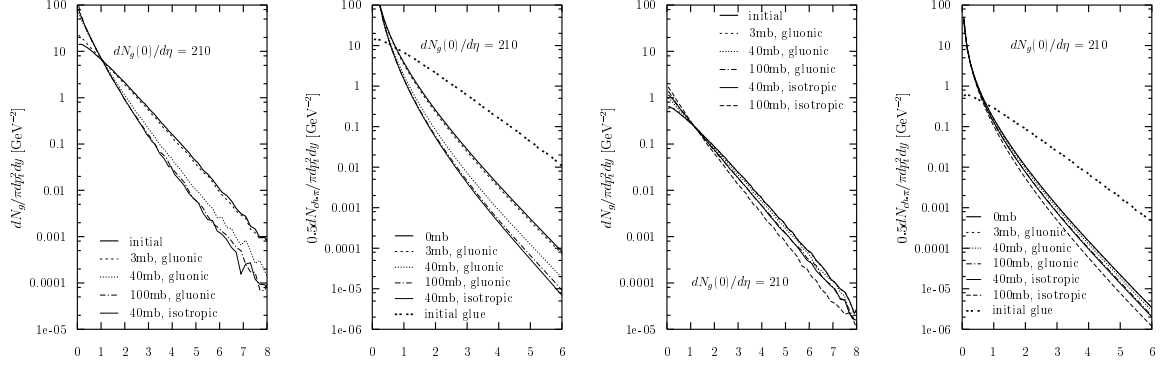


Figure 2. Final gluon and negative hadron p_{\perp} spectra (via indep. fragmentation) as a function of the elastic cross section for Au+Au at $\sqrt{s} = 130A$ GeV with $b = 6$ fm (left two plots) and $b = 12$ fm (right two plots). For local parton-hadron duality, hadron spectra are proportional to gluon spectra.

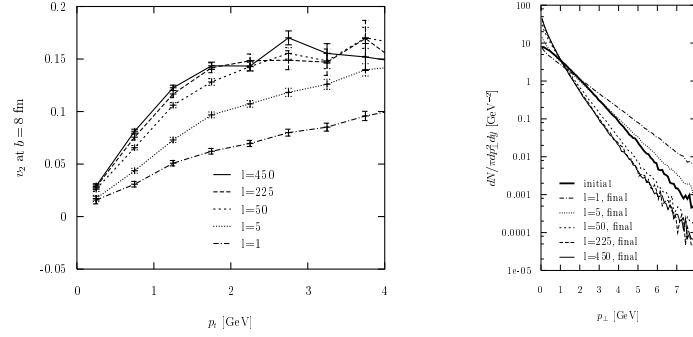


Figure 3. Gluon elliptic flow and p_{\perp} spectra for Au+Au at $\sqrt{s} = 130A$ GeV with $b = 8$ fm and particle subdivisions $\ell = 1, 5, 50, 225,$ and 450 . The elastic gg cross section was 100 mb ($\mu = T_0$).

4. X.-N. Wang, nucl-th/0009019; M. Gyulassy, I. Vitev and X.-N. Wang, nucl-th/0012092.
5. H. Sorge, Nucl. Phys. **A661**, 577 (1999) [nucl-th/9906051]; M. Bleicher and H. Stocker, hep-ph/0006147.
6. K. H. Ackermann *et al.* [STAR Collaboration], Phys. Rev. Lett. **86**, 402 (2001) [nucl-ex/0009011].
7. D. Molnar and M. Gyulassy, Phys. Rev. **C 62**, 054907 (2000) [nucl-th/0005051]. Parton cascade code MPC 1.0.6 used in the present study can be downloaded from the OSCAR homepage at <http://www.cunuke.phys.columbia.edu/OSCAR>
8. M. Gyulassy and X. Wang, Comput. Phys. Commun. **83**, (1994) 307 [nucl-th/9502021].
9. K. J. Eskola, K. Kajantie, P. V. Ruuskanen, and K. Tuominen, Nucl. Phys. **B570**, 379 (2000) [hep-ph/9909456].
10. Y. Pang, RHIC 96 Summer Study, CU-TP-815 preprint (unpublished); Generic Cascade Program (GCP) documentation available at WWW site <http://www.cunuke.phys.columbia.edu/OSCAR>
11. B. Zhang, Comput. Phys. Commun. **109**, 193 (1998) [nucl-th/9709009].
12. B. Zhang, M. Gyulassy, and Y. Pang, Phys. Rev. **C 58**, (1998) 1175 [nucl-th/9801037].
13. J. Binnewies, B. A. Kniehl and G. Kramer, Z. Phys. **C 65**, 471 (1995) [hep-ph/9407347].